Dalton Transactions

Accepted Manuscript

ROYAL SOCIETY OF CHEMISTRY

www.rsc.org/dalton

Cite this: DOI: 12.1039/c0xx00000x

www.rsc.org/xxxxxx

ARTICLE TYPE

Doubly TEMPO-coordinated gadolinium(III), lanthanum(III), and yttrium(III) complexes. Strong superexchange coupling across rare earth ion

Rina Murakami, Takeshi Nakamura, Takayuki Ishida*

Received (in XXX, XXX) Xth XXXXXXXXX 20XX, Accepted Xth XXXXXXXXX 20XX
DOI: 12.1039/b000000x

We prepared crystalline [$RE^{III}(hfac)_3(TEMPO)_2$] (RE = Gd, La, Y), where TEMPO and hfac stand for 2,2,6,6-tetramethylpiperidin-1-oxyl and 1,1,1,5,5,5-hexafluoropentane-2,4-dionate, respectively. X-Ray crystal structure of TEMPO-coordinated RE compounds was determined for the first time. The Gd and Y analogues are isomorphous, and the La derivative has a similar molecular skeleton. The Gd-O(TEMPO) bond lengths were 2.322(3) and 2.354(3) Å with the O-Gd-O angle of 140.36(11)°. The magnetic study clarified that [$Gd(hfac)_3(TEMPO)_2$] behaved as a ground S_{total} = 7/2 species. The La and Y analogues showed the superexchange interactions across the diamagnetic ions with $2J_{TEMPO1\text{-}TEMPO2}/k_B$ = –14.9(1) and –49.8(2) K, respectively. Assuming the presence of a similar interaction like the Y derivative, the Gd-TEMPO exchange couplings are estimated with $2J_{Gd\text{-}TEMPO}/k_B$ = –12.9(5) and +8.0(6) K.

Introduction

Lanthanide-based heterospin compounds have been intensively studied for development of single-molecule and single-chain magnets.[1,2] Lanthanide ions have an advantage of strong magnetic anisotropy and large spin available from the single ion origin[3] but a disadvantage of very weak magnetic exchange coupling in 4f-4f intermetallic interactions.[4] 4f-2p(π) heterospin systems[5] have been exploited to overcome the latter. Owing to the facile analysis in the studies on magneto-structure relationship[6,7] and exchange mechanism,[7-9] a spin-only Gd^{3+} ion ($4f^7$, $^8S_{7/2}$) is often chosen as an initial attempt.

To pursue stronger exchange coupling in 4f-2p systems, aliphatic nitroxides are better candidates for paramagnetic ligands than nitronyl or aromatic nitroxides. The spin localization at the N-O group is indicated by the hyperfine coupling constant a_N; for an instance, a_N = 1.5 mT for 2,2,6,6-tetramethylpiperidin-1-oxyl (TEMPO)[10] *vs.* a_N = ca. 0.75 mT for typical nitronyl nitroxides.[11] Large spin density at nitrogen and oxygen atoms affords strong exchange coupling when directly coordinated to magnetic ions.[12] Very recently, di-*tert*-butyl niroxide has been introduced as a ligand to Gd coordination chemistry.[13] The present study is focused on the application of TEMPO as an alternative 2p spin source.

Surprisingly, there has been no report on TEMPO-lanthanide coordination compounds, although the TEMPO family is widely available for spin-probe and -labeled agents.[14] We will report here the synthesis, structural characterization, and magnetic properties of a novel TEMPO-coordinated Gd^{3+} complex together with diamagnetic lanthanide ion La^{3+} ($4f^0$) and a rare earth (RE) ion Y^{3+} analogues (Scheme 1). The 1,1,1,5,5,5-hexafluoropentane-2,4-dionate anion (hfac) is used as a cap. During the study on RE/TEMPO systems, we found unexpectedly strong radical-radical superexchange coupling across a RE ion.

Scheme 1. Structural formula of **RE-TEMPO$_2$** (RE = Gd, La, Y).

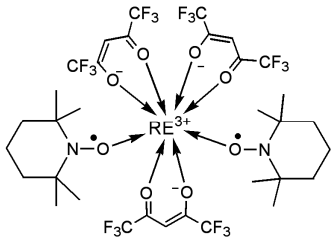

Experimental Section

Preparation of [$RE(hfac)_3(TEMPO)_2$] (RE-TEMPO$_2$). The complexation reaction was proceeded according to the method for [$Gd(hfac)_3(2pyNO)(H_2O)$] (2pyNO = *tert*-butyl 2-pyridyl nitroxide).[5] A starting material [$Gd(hfac)_3(H_2O)_2$][15] (80 mg; 0.10 mmol) was dissolved in *n*-heptane (90 mL). After being boiled and concentrated to a volume of ca. 20 mL, the solution was allowed to stand. A dichloromenthane solution (6 mL) containing 31 mg (0.20 mmol) of TEMPO (Tokyo Chemical Industry) was added to the above *n*-heptane solution while hot. The combined solution was kept in a refrigerator for two days. A yellow polycrystalline precipitate (**Gd-TEMPO$_2$**) was collected on a

filter, washed, and air-dried (48 mg; 0.044 mmol). The yield was 45%. Mp. 149–150°C (dec.). The elemental analysis (C, H, N) of the complex on a Perkin Elmer CHNS/O 2400 by a usual combustion method supported the chemical composition. Calcd.: C, 36.33; H, 3.60; N, 2.57% for $C_{33}H_{39}F_{18}GdN_2O_8$. Found: C, 36.33; H, 3.55; N, 2.75%. IR spectrum (neat; attenuated total reflection (ATR) method on a Nicolett FT-IR spectrometer) 976, 1137, 1253, 1651, 2947 cm^{-1}. **Y-TEMPO$_2$** was prepared according to the same way described above, except for the use of a starting material $[Y(hfac)_3(H_2O)_2]$ (Aldrich) in place of $[Gd(hfac)_3(H_2O)_2]$. The yield was 34%. Mp. 126-128°C (dec.). Anal. Calcd.: C, 38.76; H, 3.84; N, 2.74% for $C_{33}H_{39}F_{18}YN_2O_8$. Found: C, 39.01; H, 3.80; N, 2.97%. IR spectrum (neat; ATR) 976, 1137, 1254, 1652, 2947 cm^{-1}. **La-TEMPO$_2$** was prepared according to the same way described for **Gd-TEMPO$_2$**, except for the use of a starting material $[La(hfac)_3(H_2O)_3]$.[15] The yield was 24%. Mp. 166°C (dec.). Anal. Calcd.: C, 36.95; H, 3.67; N, 2.61% for $C_{33}H_{39}F_{18}LaN_2O_8$. Found: C, 36.78; H, 3.38; N, 2.74%. IR spectrum (neat; ATR) 978, 1132, 1250, 1649, 2948 cm^{-1}. The products were subjected to structural and magnetic studies without further purification.

X-ray crystallographic analysis. X-Ray diffraction data of **Gd-**, **Y-**, and **La-TEMPO$_2$** were collected on Rigaku R-axis Rapid and Saturn70 CCD diffractometers with graphite monochromated MoKα radiation (λ = 0.71073 Å). The structures were solved and expanded in the CRYSTALSTRUCTURE program package.[16] Numerical absorption correction was applied. All of the hydrogen atoms were located at calculated positions and the parameters were refined as a riding model. In **Gd-** and **Y-TEMPO$_2$**, there is a disorder of enantiomeric positions around a molecular pseudo two-fold axis, and the occupancy factor was optimized. Selected crystallographic data are listed in Table 1. CCDC numbers 978182, 978183, and 978184 for **Gd-**, **Y-**, and **La-TEMPO$_2$**, respectively. These data can be obtained free of charge via http://www.ccdc.cam.ac.uk/conts/retrieving.html.

Magnetic measurements. Magnetic susceptibilities of polycrystalline samples of **Gd-**, **Y-**, and **La-TEMPO$_2$** were measured on a Quantum Design MPMS-XL SQUID magnetometer in a temperature range 1.8 - 300 K. The magnetization curves were recorded in 0 – 7 T. The magnetic response was corrected with diamagnetic blank data of the sample holder obtained separately. The diamagnetic contribution of the sample itself was estimated from Pascal's constant.[17]

Results and discussion

Complexation between $[RE(hfac)_3(H_2O)_n]$ and TEMPO in a heptane-dichloromethane mixed solvent afforded **RE-TEMPO$_2$** (Scheme 1) as light yellow blocks in moderate yields. The elemental and spectral analyses support the chemical formula. We found that the use of a 1/1 molar ratio of $[RE(hfac)_3(H_2O)_n]$ and TEMPO also gave RE/TEMPO = 1/2 products. The yields were improved by using a 1/2 ratio of the starting materials for the targeted **RE-TEMPO$_2$**.

The X-ray diffraction study on **RE-TEMPO$_2$** clarified that the Gd and Y derivatives are completely isomorphous. The Gd and La derivatives crystallize in a different space group, though the molecular structures are similar to each other (Fig. 1). The RE ions are coordinated by eight oxygen atoms, consisting of two from TEMPO nitroxides and six from three diketonate groups. A whole molecule is crystallographically independent. Two TEMPO groups are located at "trans" positions with respect to the RE center, and the two TEMPO ends are well separated with three hfac groups. A spin triad is formed in **Gd-TEMPO$_2$** ($S_{R1} - S_{Gd} - S_{R2}$). Similarly, a radical pair ($S_{R1} - S_{R2}$) is found in **Y-** and **La-TEMPO$_2$**, where the diamagnetic Y^{3+} and La^{3+} may play a role of a superexchange coupler. Every molecule is magnetically isolated in a crystal, because the peripheral CF_3 and TEMPO alkyl groups work as a magnetic insulator among molecules.

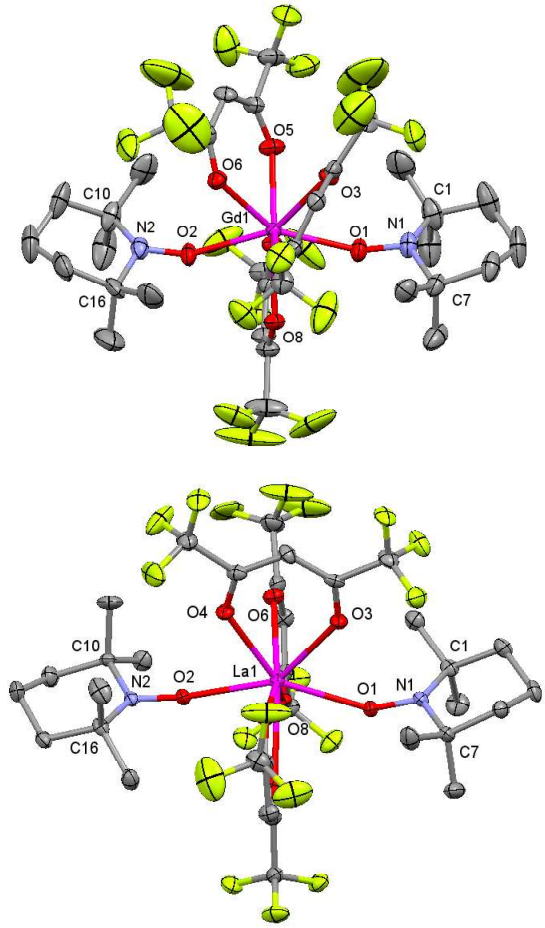

Fig. 1. Molecular structures of (a) **Gd-TEMPO$_2$** and (b) **La-TEMPO$_2$**. Thermal ellipsoids are drawn at the 50% probability level. Hydrogen atoms are omitted for clarity. A major configuration is shown in disordered hfac positions in (a).

Selected geometrical parameters are listed in Table 2. The N-O bond lengths vary in 1.288(5) – 1.299(5) Å, which are consistent with those of aliphatic neutral N-O groups.[18,19] The nitroxide oxygen atoms are directly bound to the Gd centers with the bond lengths of 2.322(3) and 2.354(3) Å for Gd1-O1 and Gd1-O2, respectively. They are shorter than those of La1–O1 and La1–O2 (2.446(3) and 2.419(4) Å, respectively) by ca. 4%. This difference is explained in terms of the normal lanthanide ionic radius contraction. On the other hand, the Gd-O bonds are longer than Y-O bonds (2.289(3) and 2.321(3) Å for Y1-O1 and Y1-O2, respectively), in agreement with the ionic radius (0.94 Å for Gd^{3+} vs 0.90 Å for Y^{3+}).[20] The ionic radius also correlates well with the cell volume in the isomorphous series.

Three hfac ligands intervene the TEMPO ends for both derivatives, and approximate molecular symmetries are different; pseudo-C_2 for **Gd-** and **Y-TEMPO$_2$** and pseudo-C_{2v} for **La-TEMPO$_2$**. Namely, for the former, one hfac is almost located on a plane approximately bisecting a molecule into two TEMPO wings and two hfac's are twisted to each other like a propeller near the plane. On the other hand, two hfac's are on and one hfac is perpendicular to the bisecting plane in the latter compound. The interatomic O1•••O2 distances are 4.399(4), 4.486(5), and 4.659(5) Å for **Gd-**, **Y-** and **La-TEMPO$_2$**, respectively, and the O1-RE1-O2 angles are 140.36(11), 140.24(11), and 146.55(13)°, respectively. Thus, we can conclude that the mutual geometries around the radical-RE-radical core would be quite similar regardless of the different hfac configuration.

The RE^{3+} ionic radii seem to be responsible for the variety of molecular structure and packing in a crystal. In our preliminary results, the crystalline solids [RE(hfac)$_3$(TEMPO)$_2$] with RE = Pr to Yb (except for Pm) were isomorphous to that of **Gd-TEMPO$_2$**.

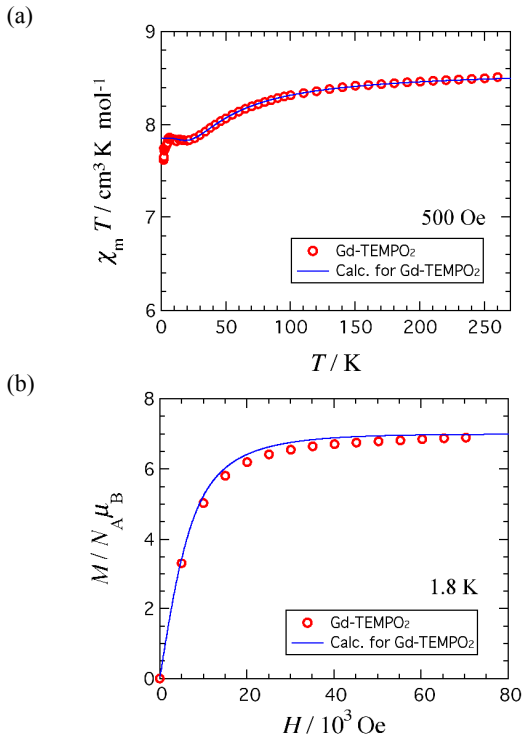

Fig. 2. (a) Temperature dependence of the product $\chi_m T$ for polycrystalline **Gd-TEMPO$_2$** measured at 500 Oe. (b) Magnetization curves for **Gd-TEMPO$_2$** measured at 1.8 K. Solid lines stand for simulated curves. For details, see the text.

The SQUID susceptometry result on polycrystalline **Gd-TEMPO$_2$** is shown in Fig. 2a. The $\chi_m T$ value was 8.51 cm^3 K mol^{-1} at 260 K, being slightly smaller than the theoretical values at the non-interacting limit from two S = 1/2 and one S = 7/2 species with g = 2 (8.63 cm^3 K mol^{-1}). On cooling, the $\chi_m T$ value decreased and reached a plateau at 7.85 cm^3 K mol^{-1} in 20 – 5 K. Note that this $\chi_m T$ value is very close to the spin-only S_{total} = 7/2 value (7.88 cm^3 K mol^{-1}). On further cooling to 1.8 K, the $\chi_m T$ value again decreased very slightly. The final drop, possibly attributed to relatively weak intermolecular antiferromagnetic coupling and/or zero-field splitting effect, seems negligible to the purpose of the present study. We pay attention to the relatively strong exchange coupling which exhibits the $\chi_m T$ decrease starting at around 150 K on cooling.

The magnetization curve was recorded at 1.8 K (Fig. 2b). The saturation magnetization is 6.9 $N_A\mu_B$, which means that **Gd-TEMPO$_2$** behaves as a S_{total} = 7/2 species. This finding is entirely consistent with the result on the $\chi_m(T)$ measurement showing the plateau in 5 – 20 K. Since the Gd^{3+} ion has S = 7/2 with g = 2, the organic spin contribution seem to be cancelled out at the ground state.

At this stage, possible spin structures are proposed for **Gd-TEMPO$_2$**. Model 1: One radical spin is ferromagnetically correlated with the Gd spin and the other antiferromagnetically. It is regarded as a strong Gd-radical coupling limit, because radical-radical interaction is not necessary. Model 2: Two radicals are antiferromagnetically coupled and their magnetic contribution is removed at low temperatures. The analysis of Gd-radical interaction would be difficult. This situation implies a strong radical-radical coupling limit.

To evaluate the interactions in **Gd-TEMPO$_2$**, we utilized an exchange coupling model involving a triangular array with 1/2 – 7/2 – 1/2 spins (Scheme 2). The radical-radical coupling is taken into consideration, and it includes a superexchange mechanism as well as a direct through-space interaction. The former seems to be dominant from the long radical-radical distance. The resultant Heisenberg spin-Hamiltonian (Eq. 1) has already been solved by Lescop and co-workers,[21] and the magnetic susceptibility is drawn as a function of temperature using the van Vleck equation.[22] Eventually the $\chi_m T$ value is calculated according to Eq. 2.

Scheme 2. Exchange-coupling model for **Gd-TEMPO$_2$**.

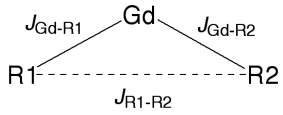

$$H = -2J_{Gd\text{-}R1}(S_{Gd}\bullet S_{R1}) - 2J_{Gd\text{-}R2}(S_{Gd}\bullet S_{R2}) - 2J_{R1\text{-}R2}(S_{R1}\bullet S_{R2}) \quad \text{Eq. 1}$$

$$\chi_m T = \frac{2N_A g_{avg}^2 \mu_B^2}{4k_B} \times \frac{35\exp(-E_1/k_BT) + 84\exp(-E_2/k_BT) + 84\exp(-E_3/k_BT) + 165\exp(-E_4/k_BT)}{3\exp(-E_1/k_BT) + 4\exp(-E_2/k_BT) + 4\exp(-E_3/k_BT) + 5\exp(-E_4/k_BT)} \quad \text{Eq. 2}$$

where

$$E_1 = \frac{9J_{Gd-R1} + 9J_{Gd-R2} - J_{R1-R2}}{2}$$

$$E_2 = \frac{J_{Gd-R1} + J_{Gd-R2} + J_{R1-R2}}{2} - \sqrt{X}$$

$$E_3 = \frac{J_{Gd-R1} + J_{Gd-R2} + J_{R1-R2}}{2} + \sqrt{X}$$

$$E_4 = \frac{-7J_{Gd-R1} - 7J_{Gd-R2} - J_{R1-R2}}{2}$$

and

$$X = 16J_{Gd-R1}^2 + 16J_{Gd-R2}^2 + J_{R1-R2}^2 - 31J_{Gd-R1}J_{Gd-R2} - J_{Gd-R1}J_{R1-R2} - J_{Gd-R2}J_{R1-R2}$$

The parameters were optimized from the data of Fig. 2a, to give $2J_{R1\text{-}R2}/k_B$ = –88(27) K and g_{avg} = 1.988(1) with unsuccessful convergence of $J_{Gd\text{-}R1}$ or $J_{Gd\text{-}R2}$. Apparently, this solution realizes Model 2. The magnitude of $J_{R1\text{-}R2}$ seem to be somewhat large

from the long distance between the two nitroxide oxygen atoms (4.389(6) Å). To examine the exchange couplings in detail, we moved to investigate a reference compound with the 4f spin masked.

The magnetic susceptibility of **La-TEMPO$_2$** was measured, and the result is displayed in Fig. 3. The $\chi_m T$ value of **La-TEMPO$_2$** was 0.71 cm^3 K mol^{-1} at 260 K, being slightly smaller that the theoretical value of two non-interacting S = 1/2 species with g = 2 (0.75 cm^3 K mol^{-1}). On cooling, the $\chi_m T$ value monotonically decreased, indicating the presence of dominant antiferromagnetic coupling. The Bleaney-Bowers equation[23] based on a singlet-triplet model ($H = -2J_{R1\text{-}R2}(S_{R1}\bullet S_{R2})$) was successfully applied to this data, affording $2J_{R1\text{-}R2}/k_B$ = –14.9(1) K with g = 1.951(2). The simulated $\chi_m T(T)$ curve well reproduced the experimental data. The purity factor is 95% estimated from the ideal g = 2.

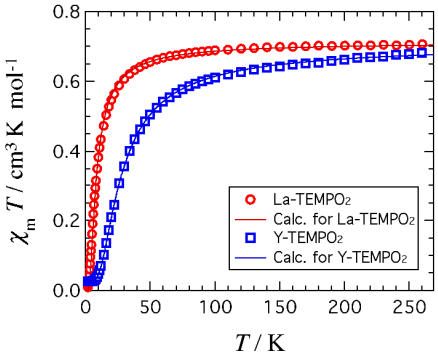

Fig. 3. Temperature dependence of the product $\chi_m T$ for polycrystalline **La-** and **Y-TEMPO$_2$**measured at 5000 Oe. Solid lines stand for simulated curves based on the Bleaney-Bowers equation. For the parameters, see the text.

We deliberately examined another instance having a radical-RE-radical chromophore, and actually have found stronger magnetic coupling in the Y derivative. The magnetic susceptibility of **Y-TEMPO$_2$** was similarly measured, and the $\chi_m T$ vs T result has been superposed in Fig. 3. The $\chi_m T$ value was 0.69 cm^3 K mol^{-1} at 260 K, and on cooling, the $\chi_m T$ value monotonically decreased and reached an almost plateau in 6 – 2 K, indicating the presence of notably strong antiferromagnetic coupling. The Bleaney-Bowers analysis gave $2J_{R1\text{-}R2}/k_B$ = –49.8(2) K with g = 1.945(1). The simulated $\chi_m T(T)$ curve well reproduced the experimental data. The $\chi_m T$ plateau below 6 K has a value of 0.027 cm^3 K mol^{-1}, which implies the presence of a doublet impurity of 3.6%. The flat $\chi_m T$ profile in this region guarantees that the intermolecular interaction would be negligible.

The radical-radical superexchange interaction across the La^{3+} and Y^{3+} ions[24] are successfully determined as $2J_{R1\text{-}R2}/k_B$ = –14.9(1) and –49.8(2) K, respectively. These values were considerably large, viewing from the long O1•••O2 distances (4.659(5) and 4.486(5) Å, respectively). Gatteschi and co-workers reported the radical-radical interaction of $2J/hc$ = –4.5 cm^{-1} in the infinite linear complex [Y(hfac)$_3$NITEt] (NITEt stands for 2-ethyl-4,4,5,5-tetramethyl-4,5-dihydro-1*H*-imidazol-1-yloxyl 3-oxide).[25] The corresponding value of **Y-TEMPO$_2$** is ca. 8 times larger than that of [Y(hfac)$_3$NITEt], and this factor is partly explained in terms of the spin densities at the radical oxygen atoms.

The Gd^{3+} and La^{3+} (or Y^{3+}) have different numbers of 4f electrons, and the 4f electrons might play a role in the superexchange through them. Superexchange coupling is described on the basis of electron-transfer from ligand to metal or from metal to ligand,[26] so that the exchange would depend on the electron configuration at the bridging ion. However, as an approximation, we applied the $J_{R1\text{-}R2}$ values of **Y-** and **La-TEMPO$_2$** to that of **Gd-TEMPO$_2$** to understand the nature of the Gd-radical interactions.

Thus, parameter optimization was performed according to Eq. 2, with $J_{R1\text{-}R2}$ frozen and $J_{Gd\text{-}R1}$, $J_{Gd\text{-}R2}$, and g_{avg} adjustable. The crystallographic study reveals that the Gd and Y analogues are isomorphous, and accordingly applying the value of **Y-TEMPO$_2$** seems to be plausible. The optimization from the data of Fig. 2a using $2J_{R1\text{-}R2}/k_B$ = –49.8 K gave $2J_{Gd\text{-}R1}/k_B$ = –12.9(5) K and $2J_{Gd\text{-}R2}/k_B$ = +8.0(6) K with g_{avg} = 1.9972(3). The simulated curve very well reproduced the experimental data, and in particular a very gradual $\chi_m T$ increase on cooling from 20 to 5 K was satisfactorily fit. Moreover, the simulated $M(H)$ curve[21] with the same parameters also reproduced the experimental magnetization (Fig. 2b). The only slightly downward deviation of the experimental data may be found, which is rationalized by taking into consideration the final $\chi_m T$ drop at the lowest temperature region in the $\chi_m T(T)$ plot (Fig. 2a). The present argument allows a possible explanation based on Model 1. Each TEMPO radical is ferro- or antiferromagnetically correlated to the Gd center in a molecule.

One may wonder how about the $J_{R1\text{-}R2}$–dependence of $J_{Gd\text{-}R1}$ and $J_{Gd\text{-}R2}$. To check this by simulation, another calculation was done with an assumption of $2J_{R1\text{-}R2}/k_B$ = –14.9 K from **La-TEMPO$_2$**. We obtained $2J_{Gd\text{-}R1}/k_B$ = –19.7(6) K and $2J_{Gd\text{-}R2}/k_B$ = +15.0(8) K with g_{avg} = 1.9959(4). From the comparison between the two calculations, though the magnitudes were varied to some extent, a combination of moderate ferromagnetic and antiferromagnetic couplings is retained.

Finally, we make a comment on assignment. In the Gd-nitroxide family, we have proposed the charge-transfer mechanism of the nitroxide π^* electron to empty Gd 5d orbitals to explain the ferromagnetic Gd-nitroxide coupling often observed.[7] The Gd-O-N-C torsion is known to be a convenient indicator for displacement of the Gd ion from the nitroxide π* nodal plane. The empirical relation tells us that smaller torsion favors stronger antiferromagnetic coupling.[7,27] Actually, both torsion angles were measured for the O1-N1 and O2-N2 groups, but they fell in a narrow region of 97 – 104° (Table 2). Appreciable differences were found in the Gd-O bond lengths (2.313(5) *vs.* 2.360(4) Å) and the Gd-O-N bond angles (154.1(4) *vs.* 147.5(4)°). Unfortunately, we have no magneto-structural relation with respect to these parameters and hardly solve this assignment problem.

The exchange parameters $J_{R1\text{-}R2}$, $J_{Gd\text{-}R1}$, and $J_{Gd\text{-}R2}$ are comparable in magnitude, being incompatible with the strong Gd-radical or radical-radical coupling limit. When the geometries on both radical sides are similar and an isosceles triangular model would be plausible ($J_{Gd\text{-}R1} \approx J_{Gd\text{-}R2}$), antiferromagnetic $J_{R1\text{-}R2}$ might give rise to frustration. In fact, the symmetry is broken, and

one Gd-radical geometry takes on the role of a ferromagnetic coupler. The strong TEMPO•••TEMPO interaction seems to be responsible for the coexistence of the ferro- and antiferromagnetic couplings in the Gd-TEMPO interaction.

Summary

We have structurally and magnetically characterized **Gd-**, **Y-**, and **La-TEMPO$_2$**. To our knowledge, there has been only one example of the radical-lanthanide coordination compounds when the radical is a bisaliphatic nitroxide.[13] The present study offers a novel three-centered 2p-4f-2p heterospin system using an aliphatic nitroxide. Relatively strong 4f-2p exchange couplings are realized from our molecular design. A few guiding principles for constructing 4f-2p coupled systems are known and applicable,[7] and at the same time 2p-2p interactions must not be ignored. Superexchange interactions across RE ions have been practically uncultivated before our work. The study on the correlation between the structures and magnetic properties of 2p-2p interactions as well as 4f-2p ones is of increasing importance to explore 4f-2p-based molecular magnets.

Acknowledgments

Authors thank Mr. Takuya Kanetomo for assistance in the magnetic measurements. This work was partly supported by KAKENHI (Grant Number JSPS/22350059).

Notes and references

Department of Engineering Science, The University of Electro-Communications, Chofu, Tokyo 182-8585, Japan. Fax: 81 42 443 5501; Tel: 81 42 443 5490; E-mail: ishi@pc.uec.ac.jp

1 (a) S. Osa, T. Kido, N. Matsumoto, N. Re, A. Pochaba and J. Mrozinski, *J. Am. Chem. Soc.,* 2004, **126**, 420; (b) F. Pointillart, K. Bernot, R. Sessoli and D. Gatteschi, *Chem. -Eur. J.*, 2007, **13**, 1602; (c) L. Bogani, C. Sangregorio, R. Sessoli and D. Gatteschi, *Angew. Chem. Int. Ed.*, 2005, **44**, 5817.

2 (a) F. Mori, T. Ishida and T. Nogami, *Polyhedron*, 2005, **24**, 2588; (b) F. Mori, T. Nyui, T. Ishida, T. Nogami, K.-Y. Choi and H. Nojiri, *J. Am. Chem. Soc.*, 2006, **128**, 1440; (c) S. Ueki, T. Ishida, T. Nogami, K.-Y. Choi and H. Nojiri, *Chem. Phys. Lett.*, 2007, **440**, 263.

3 N. Ishikawa, M. Sugita, T. Ishikawa, S.-y. Koshihara and Y. Kaizu, *J. Am. Chem. Soc.*, 2003, **125**, 8694.

4 L. Canadillas-Delgado, J. Pasan, O. Fabelo, M. Julve, F. Lloret and C. Ruiz-Perez, *Polyhedron*, 2013, **52**, 321.

5 R. Murakami, T. Ishida, S. Yoshii and H. Nojiri, *Dalton Trans.*, 2013, **42**, 13968.

6 (a) J. P. Costes, F. Dahan and A. Dupis, *Inorg. Chem.*, 2000, **39**, 5994; (b) R. E. P. Winpenny, *Chem. Soc. Rev.,* 1998, **27**, 447.

7 T. Ishida, R. Murakami, T. Kanetomo and H. Nojiri, *Polyhedron*, 2013 **66**, 183.

8 (a) M. Andruh, I. Ramade, E. Codjovi, O. Guillou, O. Kahn and J. C. Trombe, *J. Am. Chem. Soc.*, 1993, **115**, 1822; (b) I. Ramade, O. Kahn, Y. Jeannin and F. Robert, *Inorg. Chem.*, 1997, **36**, 930.

9 G. Rajaraman, F. Totti, A. Bencini, A. Caneschi, R. Sessoli and D. Gatteschi, *Dalton Trans.*, **2009**, 3153.

10 O. H. Griffith, D. W. Cornell and H. M. McConnell, *J. Chem. Phys.*, 1965, **43**, 2909.

11 (a) J. Goldman, T. E. Petersen, K. Torssell and J. Becher, *Tetrahedron*, 1973, **29**, 3833; (b) E. F. Ullman, J. H. Osiecki, G. B. Boocock and R. Darcy, R. *J. Am. Chem. Soc.*, 1972, **94**, 7049.

12 H. M. McConnell, *J. Chem. Phys.*, 1963, **39**, 1910.

13 T. Kanetomo and T. Ishida, *Chem. Commun.*, 2014, in press. DOI:10.1039/C3CC48326F.

14 (a) G. I. Likhtenshtein, J. Yamauchi, S. Nakatsuji, A. I. Smirnov and R. Tamura, *Nitroxides: Applications in Chemistry, Biomedicine, and Materials Science*, Wiley-VCH, Weinheim (2008); (b) L. J. Berliner, *Spin-Labeling: Theory and Applications*, Academic Press, New York, (1976); (c) J. F. Keana, *Chem. Rev.*, 1978, **78**, 37.

15 M. F. Richardson, W. F. Wagner and D. E. Sands, *J. Inorg. Nucl. Chem.*, 1968, **30**, 1275.

16 CRYSTALSTRUCTURE version 4.0, Rigaku Corp., Tokyo, Japan (2010).

17 O. Kahn, *Molecular Magnetism*; VCH: Weinhein, 1993. Chapter 1, Table I.1.

18 A. Okazawa, Y. Nagaichi, T. Nogami and T. Ishida, *Inorg. Chem.*, 2008, **47**, 8859.

19 (a) F. Iwasaki, J. H. Yoshikawa, H. Yamamoto, E. Kan-nari, K. Takada, M. Yasui, T. Ishida and T. Nogami, *Acta Crystallogr.*, 1999, **B55**, 231; (b) F. Iwasaki, J. H. Yoshikawa, H. Yamamoto, K. Takada, E. Kan-nari, M. Yasui, T. Ishida and T. Nogami, *Acta Crystallogr.*, 1999, **B55**, 1057.

20 (a) R. D. Shannon and C. T. Prewitt, *Acta Crystallogr., Sect. B: Struct. Crystallogr. Cryst. Chem.*, 1969, **25**, 925; (b) R. D. Shannon, *Acta Crystallogr., Sect. A: Cryst. Phys., Diffr., Theor. Gen. Cryst.*, 1976, **32**, 751.

21 C. Lescop, E. Belorizky, D. Luneau and P. Rey, *Inorg. Chem.*, 2002, **41**, 3375.

22 E. Sinn, *Coord. Chem. Rev.*, 1970, **5**, 313.

23 B. Bleaney and D. K. Bowers, *Proc. R. Soc. (London) Ser. A*, 1952, **214**, 451.

24 K. Koide and T. Ishida, *Inorg. Chem. Commun.*, 2011, **14**, 194.

25 C. Benelli, A. Caneschi, D. Gatteschi, L. Pardi and P. Rey, *Inorg. Chem.*, 1989, **28**, 3230.

26 (a) P. W. Anderson, *Phys. Rev.*, 1959, **115**, 2; (b) J. B. Goodenough, *Phys. Rev.*, 1955, **100**, 564; (c) J. Kanamori, *J. Phys. Chem. Solids*, 1959, **10**, 87.

27 (a) A. Caneschi, A. Dei, D. Gatteschi, L. Sorace and K. Vostrikova, *Angew. Chem. Int. Ed.*, 2000, **39**, 246; (b) J. R. Rinehart, M. Fang, W. J. Evans and J. R. Long, *Nature Chem.*, 2011, **3**, 538.

Cite this: DOI: 12.1039/c0xx00000x

www.rsc.org/xxxxxx

ARTICLE TYPE

Table 1. Selected crystallographic data for **RE-TEMPO$_2$**.

Compounds	**Gd-TEMPO$_2$**	**Y-TEMPO$_2$**	**La-TEMPO$_2$**
Formula	$C_{33}H_{39}F_{18}GdN_2O_8$	$C_{33}H_{39}F_{18}N_2O_8Y$	$C_{33}H_{39}F_{18}LaN_2O_8$
Formula weight	1090.90	1022.56	1072.56
Habit	yellow blocks	yellow blocks	yellow blocks
Dimension /mm^3	0.39 × 0.32 × 0.27	0.74 × 0.45 × 0.41	0.24 × 0.13 × 0.12
T / K	100	100	100
Crystal system	monoclinic	monoclinic	triclinic
Space group	$P2_1/c$	$P2_1/c$	P-1
a /Å	11.992(3)	11.968(6)	9.3813(17)
b /Å	16.147(3)	16.162(9)	11.977(3)
c /Å	22.318(5)	22.260(11)	21.854(5)
α/°	90	90	74.842(9)
β /°	91.041(10)	91.08(4)	78.118(9)
γ /°	90	90	66.457(9)
V /Å^3	4320.7(15)	4305(4)	2158.5(8)
Z	4	4	2
D_{calc} /g cm^{-3}	1.677	1.578	1.650
Unique data	9791	9714	9557
μ(MoKα) /mm^{-1}	1.664	1.578	1.110
R (F)[a] ($I > 2\sigma(I)$)	0.0533	0.0645	0.0662
$R_w(F^2)$[b] (all data)	0.0574	0.0672	0.0742
G.O.F.	1.088	1.068	1.077

[a] $R = \Sigma \, ||F_o| - |F_c|| / \Sigma \, |F_o|$. [b] $R_w = [\Sigma \, w(F_o^2 - F_c^2)^2 / \Sigma \, w(F_o^2)^2]^{1/2}$.

Cite this: DOI: 12.1039/c0xx00000x

www.rsc.org/xxxxxx

ARTICLE TYPE

Table 2. Selected geometrical parameters for **RE-TEMPO$_2$**.

Compounds	**Gd-TEMPO$_2$**	**Y-TEMPO$_2$**	**La-TEMPO$_2$**
Bond lengths, d / Å			
RE1–O1	2.322(3)	2.289(3)	2.446(3)
RE1–O2	2.354(3)	2.321(3)	2.419(4)
RE1–O(hfac)	2.360(3) – 2.399(3)	2.327(4) – 2.362(3)	2.476(4) – 2.524(5)
O1–N1	1.288(5)	1.299(5)	1.292(6)
O2–N2	1.289(5)	1.293(5)	1.289(5)
N1–C1	1.500(7)	1.488(7)	1.497(7)
N1–C7	1.502(6)	1.501(6)	1.495(7)
N2–C10	1.497(6)	1.500(6)	1.496(7)
N2–C16	1.502(6)	1.500(7)	1.500(7)
Bond angles, θ / °			
RE1–O1–N1	154.5(3)	154.7(3)	146.0(4)
RE1–O2–N2	147.6(3)	148.8(3)	171.1(4)
O1–RE1–O2	140.36(11)	140.24(11)	146.55(13)
O1–N1–C1	115.6(4)	115.3(4)	115.4(4)
O1–N1–C7	115.1(4)	115.0(4)	115.8(5)
C1–N1–C7	125.5(4)	125.8(4)	125.7(4)
O2–N2–C10	115.7(4)	115.7(4)	115.7(5)
O2–N2–C16	116.0(4)	116.3(4)	115.7(4)
C10–N2–C16	124.3(4)	124.4(4)	125.6(4)
Torsion angles, ϕ / °			
RE1–O1–N1–C1	–99.6(6)	124.4(4)	–96.6(5)
RE1–O1–N1–C7	101.2(6)	101.1(6)	102.2(6)
RE1–O2–N2–C10	102.8(5)	101.6(5)	– [a)]
RE1–O2–N2–C16	–98.4(5)	–98.9(5)	– [a)]

[a)] Unavailable because of the large La1-O2-N2 bond angle.

A Graphical Contents Entry

X-Ray crystal structure of TEMPO-coordinated lanthanide compounds was determined for the first time. The magnetic study clarified that $[Gd(hfac)_3(TEMPO)_2]$ behaved as a ground S_{total} = 7/2 species. The La and Y analogues showed the superexchange interactions across the diamagnetic ions with $2J_{TEMPO1\text{-}TEMPO2}/k_B$ = –14.9(1) and –49.8(2) K, respectively.